

Distribution and Energies of Grain Boundaries in Magnesia as a Function of Five Degrees of Freedom

David M. Saylor,^{*,†} Adam Morawiec,[‡] and Gregory S. Rohrer^{*}

Materials Science and Engineering Department, Carnegie Mellon University, Pittsburgh, Pennsylvania 15213

The multiplicity of distinct grain boundary configurations in polycrystals has made it difficult to determine the relative frequency with which each configuration is adopted. As a result, the physiochemical properties of each boundary and the influence of the distribution of boundaries on macroscopic materials properties are not well understood. Using a semiautomated system, we have measured all five macroscopically observable degrees of freedom of 4.1×10^6 boundary plane segments making up $5.2 \times 10^6 \mu\text{m}^2$ of grain boundary interface area in a magnesia polycrystal. Our observations demonstrate that not all grain boundary configurations occur with the same frequency and that the relative free energies of the different interfacial configurations influence the population distribution. Furthermore, the results indicate that relative grain boundary energies can be estimated based on the free surface energies.

I. Introduction

DISTINCT grain boundary configurations in centrosymmetric crystals can be discriminated based on their five macroscopic degrees of freedom: three describe the misorientation between the adjacent crystallites and two describe the orientation of the boundary plane separating the two crystals.¹ Because the domain of boundary types is five-dimensional, the number of distinguishable boundary configurations that can occur in nature is too large to be practically sampled by traditional microscopies that require the continuous attention of a human operator. For example, if one resolves the macroscopically observable parameters of grain boundaries in a cubic material with 5° of resolution, then there are $\sim 2 \times 10^5$ distinct configurations.² The result of this natural complexity is that little is known about how grain boundaries in real polycrystals occupy the possible configurational states or how the physical and chemical properties of boundaries vary with configuration.

The purpose of this communication is to demonstrate that automated microscopic analysis can now be used to overcome the difficulty of sampling large numbers of grain boundaries. We have measured all five degrees of freedom of 4.1×10^6 grain boundary plane segments in a magnesia polycrystal and present here a brief overview of the methods used and the principal findings. Our analysis demonstrates that there is significant texture in the space

of grain boundary orientations and that boundaries are configured to achieve relatively low energies.

II. Experimental Method

The preparation and characteristics of the magnesia specimen used for this study have already been described in detail.³ Briefly, the sample was hot-pressed at 1700°C , annealed for 48 h at 1600°C , and had a grain size of $109 \mu\text{m}$. The grain boundary positions were revealed by thermally etching the polished surface at 1400°C in air. Grain boundary configurations were determined using a combination of scanning electron microscope (SEM) images and electron backscattered diffraction patterns (EBSPs) automatically acquired at regular intervals on the sample surface. The SEM images were recorded in slightly overlapping regions to determine the boundary positions and the EBSPs were recorded periodically to determine the grain orientations. The pixel resolution in the SEM images was $0.25 \mu\text{m}$ and the spacing between grain orientation measurements was $8 \mu\text{m}$. After a surface area of $\sim 6 \text{ mm} \times 1.5 \text{ mm}$ was characterized in this way, a known thickness of material (averaging $7 \mu\text{m}$) was removed by polishing. This process was repeated to accumulate data from five layers.

The microscopic data must be analyzed in a global reference frame. After correcting for the instrumental distortions of the images and grain orientation maps, a reference frame was established for each layer by considering the correlations in the overlapping regions.⁴ Grain orientations were assigned based on the individual EBSPs in the same area. After rejecting anomalous measurements, final assignments were made by averaging the individual orientation measurements within each grain. The parallel sections in the data set were fixed in a single reference frame using a transformation that maximizes the area of overlap between positions in adjacent layers having the same orientation. By comparing the spatial overlap of grains with similar orientations on adjacent layers, it was possible to identify parts of single grains in different planar sections; more than 5000 distinct grains were identified in this way. Finally, common grain boundaries on adjacent layers were used to create a meshed interfacial surface. Every fourth pixel along a boundary served as the vertex of one of 4.1×10^6 triangular elements. Each element represents an observed grain boundary plane segment for which the orientation of the boundary and the misorientation across the boundary are known.

The five-dimensional space of grain boundary types was discretized into 6561 distinguishable configurations. The symmetry and inhomogeneity of the space were considered so that each discrete configuration was associated with the same volume of the space.⁵ This was accomplished by using three Euler angles (ϕ_1 , Φ , and ϕ_2) to describe the misorientation and two spherical angles (θ , ϕ) to describe the boundary plane normals. The misorientation parameters— ϕ_1 , $\cos \Phi$, and ϕ_2 —range from 0 to $\pi/2$, 1, and $\pi/2$, respectively, and were discretized in units of $\Delta\phi_1 = 10^\circ$, $\Delta(\cos \Phi) = 1/9$, and $\Delta\phi_2 = 10^\circ$. The boundary plane parameters, $\cos \theta$ and ϕ , range from 0 to 1 and 2π , respectively, and were discretized in units of $\Delta(\cos \theta) = 1/9$ and $\Delta\phi = 10^\circ$. This scheme, which

D. Wolf—contributing editor

Manuscript No. 187191. Received January 23, 2002; approved September 12, 2002.

This work was supported primarily by the MRSEC program of the National Science Foundation under Award Number DMR-0079996.

^{*}Member, American Ceramic Society.

[†]Current address: National Institute of Standards and Technology, Gaithersburg, Maryland.

[‡]Instytut Metalurgii i Inżynierii Materiałowej PAN, Reymonta 25, 30-059 Krakow, Poland.

creates equal volume partitions in the five-dimensional space, also leads to discrete grain boundary configurations that span different ranges of the angular parameters. However, on average the angular resolution was 10° for each of the five parameters. After the area of each observed grain boundary plane was added to its corresponding discrete configuration, the results were normalized by the total area so that the sum in each partition is a multiple of a random distribution (MRD).

III. Results

To view the observed distribution in the five-dimensional space of grain boundary configurations, a fixed misorientation is chosen based on an axis-angle pair, and the distribution of boundary orientations is plotted on a stereographic projection. For example, the data illustrated in Fig. 1(a) show the distribution of grain boundary orientations for all boundaries with a 35° misorientation about the $[110]$ axis. As expected, the grain boundary planes are not distributed randomly. While the observed distribution is different for different axis-angle combinations, the relative population of the different boundary orientations at any specific point in misorientation space always varies by more than a factor of 2. For brevity, the discussion in this communication will be limited to the features in Fig. 1(a) that are characteristic of the grain boundary plane distribution at all points in misorientation space.

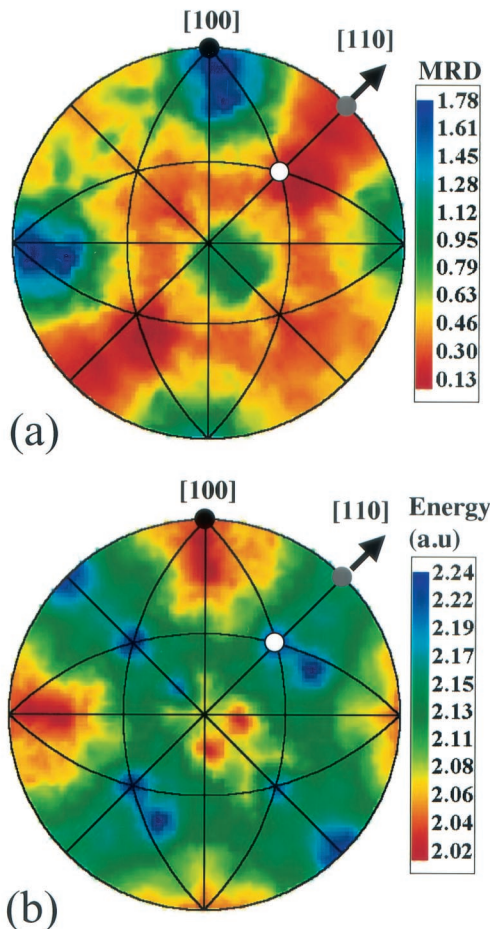


Fig. 1. (a) The observed distribution of grain boundary planes, plotted in stereographic projection for a misorientation of 35° around the $\langle 110 \rangle$ axis, which lies in the plane of projection. The $\{100\}$, $\{110\}$, and $\{111\}$ orientations are marked with black, gray, and white circles, respectively. The mirror plane perpendicular to the axis of misorientation results from the combined effect of the diad along $[110]$ and the inversion symmetry of the bicrystals. (b) Hypothetical grain boundary energies for the same configurations derived from the surface energies.

The results in Fig. 1(a) show that $\{100\}$ grain boundary planes occur more frequently than any other type. In fact, for all misorientations greater than 15° , the maximum in the grain boundary distribution always occurs at $\{100\}$. For smaller misorientation angles, the $\{110\}$ type planes are also highly populated. While we do not intend to discuss the low-angle boundaries further in this communication, the high population of $\{110\}$ planes is thought to be connected to dislocation structures at the interface.⁶ When the geometrically necessary dislocation density is calculated according to Frank's equation,⁷ we find the minimum dislocation density for boundaries with $\{110\}$ planes.

The spreading of the maxima in Fig. 1(a) is easily understood when one considers the interface geometry. Note that when the misorientation is fixed and one member of a bicrystal pair is terminated by a $\{100\}$ plane, the index of the geometrically required complement will have to differ from $\{100\}$ by the misorientation angle, in this case, 35° . The presence of these boundary complements explains the spreading of the maxima away from $\{100\}$.

The illustrations in Fig. 2, constructed using all of the observed grain boundary segments, clearly demonstrate that $\{100\}$ boundary planes are preferred throughout misorientation space. Figure 2(a) shows that the grain boundary population, normalized to remove misorientation texture bias, increases as the minimum angular deviation of the two boundary plane normals from $\langle 100 \rangle$ decreases. If the grain boundary planes predominantly have $\{100\}$ orientations, then their lines of intersection (triple lines) must also show a preference for $\langle 100 \rangle$ directions. This is confirmed in Fig. 2(b).

One possible explanation for the predominance of boundaries with $\{100\}$ orientations is that such boundaries have a relatively

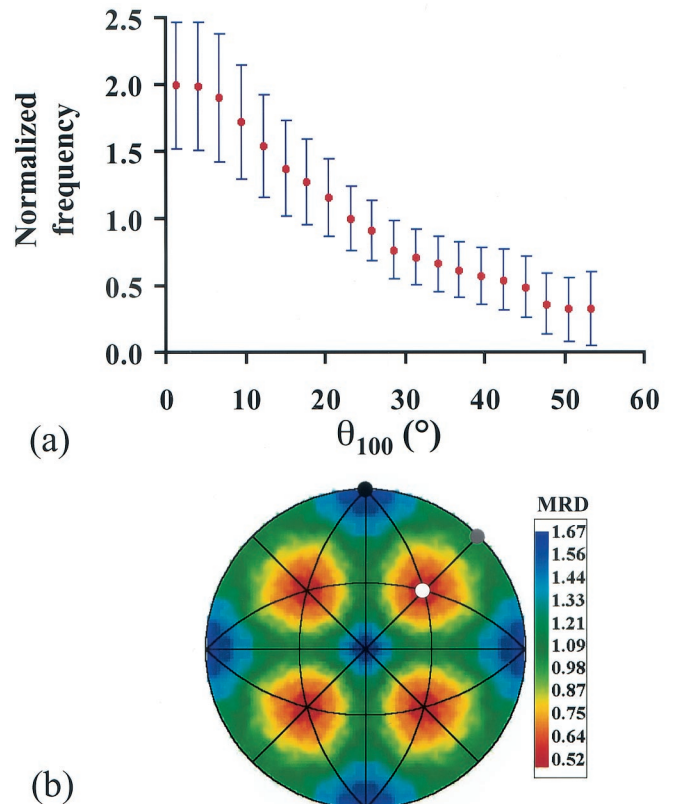


Fig. 2. (a) Normalized values of the grain boundary population as a function of the minimum angular deviation of the two boundary plane normals from $\langle 100 \rangle$, θ_{100} . At each value of θ_{100} , the average of all normalized values within a 2.74° range is represented by the point; the bars indicate 1 standard deviation above and below the mean. (b) Stereographic projection of the crystallographic distribution of triple line directions. The $[100]$, $[110]$, and $[111]$ directions are marked with black, gray, and white circles, respectively.

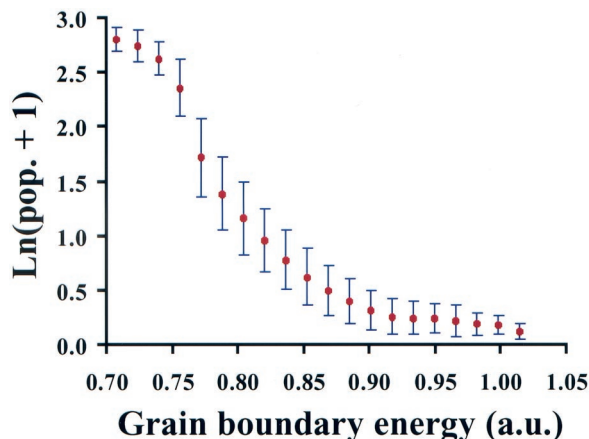


Fig. 3. Normalized values of the grain boundary population as a function of the reconstructed grain boundary energy. The average of all normalized values within a range of 0.016 au is represented by the point; the bars indicate 1 standard deviation above and below the mean.

lower energy and that during the extended high-temperature anneal, boundaries in the sample adopted configurations that minimize the total grain boundary energy. To test this idea, the energies reconstructed from observations of grain boundary triple junctions can be compared with the grain boundary distribution. In this data set, there were 1.9×10^4 triple junctions. By assuming the Herring⁸ condition of local equilibrium and applying the capillarity vector reconstruction method, it is possible to estimate the relative energies over all five degrees of freedom.⁹ The results from this process, which will be described in detail elsewhere, show that {100} boundaries have relatively low energies. We used the Spearman rank-order correlation coefficient¹⁰ to measure the degree of correlation between the normalized population of grain boundaries and the reconstructed grain boundary energy throughout the entire data set. Values of this correlation coefficient range from -1 to 1 , which indicate perfect inverse and direct correlation, respectively. The intermediate point, 0 , indicates no correlation. In this case, the correlation coefficient between the observed population of different configurations and the grain boundary energy was -0.77 . This is a substantial inverse correlation.

The relationship between the population and the reconstructed energies can be illustrated by plotting the mean occupancy of boundary configurations with the same energy (see Fig. 3). The plot convincingly demonstrates that grain boundary configurations with relatively high energies are underpopulated while low-energy configurations are more numerous. Based on this observation, we hypothesize that the microstructure of our sample, which resulted from extensive grain growth at 1600°C , has adopted configurations in the five-dimensional space that minimize the total grain boundary energy.

IV. Discussion

Perhaps the most intriguing question to arise from these data is, what is the fundamental basis for the relatively low energy of {100} boundaries? Interestingly, earlier measurements of the orientation dependence of the surface energy of magnesia, conducted in our lab on the same sample, indicated that the (100) plane has the minimum energy. The energies of the (110) and (111) surfaces are 7% and 17% higher than (100), respectively.¹¹ The ordering of these energies is consistent with the assumption that the surface energy is proportional to the density of broken bonds. If we assume that the excess free energy of a high-angle grain boundary also originates primarily from the broken bonds, then it follows that the grain boundary energy should be related to the energies of the free surfaces that bound the crystals on either side of the boundary. Specifically, we can adopt the idea originally

proposed by Wolf¹² that the grain boundary energy is the sum of the two surface energies that make up this boundary, minus a binding energy that reflects the energy returned when bonds across the boundary are reformed. For general boundaries, where the repeat units of the two free surfaces do not form a commensurate structure and the misorientation cannot be created by a set of nonoverlapping dislocations, the density of reformed bonds and, therefore, the binding energy should be constant. This indicates that the anisotropy of the sum of the two free surface energies represents the anisotropy of the energy of general boundaries.

When the energy anisotropy of the grain boundaries, as represented by the sum of the two surface energies, is compared with the boundary distribution, a substantial inverse correlation is observed. For example, in Fig. 1(b), the anisotropy predicted from the sum of the two surface energies is compared with the observed distribution of boundaries with a 35° misorientation about the $\langle 110 \rangle$ axis. To demonstrate that the inverse correlation apparent in Fig. 1 is persistent throughout the data set, we have again used the Spearman rank-order correlation coefficient¹⁰ and found that the correlation of the boundary population and hypothetical energies is -0.76 .

V. Conclusions

Our observations of the distribution and energies of grain boundaries have several interesting consequences. First, there are preferred orientations for grain boundary planes in MgO. Second, the population distribution exhibits a substantial inverse correlation with the grain boundary energy. This suggests that during grain growth, boundaries configure their orientations not only to maintain local equilibrium at the triple lines, but also to minimize the total grain boundary energy. Surprisingly, the variations in the energies of general boundaries correlate well to a model based on the free surface energies of the constituent planes. This result suggests that the energies of grain boundaries, like the energies of free surfaces, are strongly influenced by the density of broken bonds that are required to form the interface. Examining the generality of this conclusion is one of the potential applications for this new method of grain boundary texture analysis.

References

- ¹C. Goux, "Structure des Joints de Grains: Considérations Cristallographiques et Méthodes de Calcul des Structures," *Can. Metall. Q.*, **13** [1] 9–31 (1974).
- ²D. M. Saylor, A. Morawiec, B. L. Adams, and G. S. Rohrer, "Misorientation Dependence of the Grain Boundary Energy in Magnesia," *Interface Sci.*, **8** [2/3] 131–40 (2000).
- ³D. M. Saylor, D. E. Mason, and G. S. Rohrer, "Experimental Method for Determining Surface Energy Anisotropy and its Application to Magnesia," *J. Am. Ceram. Soc.*, **83** [5] 1226–32 (2000).
- ⁴S. Mahadevan and D. Casasent "Detection of Triple Junction Parameters in Microscope Images"; pp. 204–14 in Proceedings of SPIE—The International Society for Optical Engineering, Vol. 4387, *Optical Pattern Recognition XII*. Edited by D. P. Casasent and T.-H. Chao. International Society for Optical Engineering, Bellingham, WA, 2001.
- ⁵A. Morawiec, "Symmetries of Grain Boundaries"; pp. 509–14 in *Proceedings of the Third International Conference on Grain Growth*. Edited by H. Weiland, B. L. Adams, and A. D. Rollett. TMS, Warrendale, PA, 1998.
- ⁶W. T. Read and W. Shockley, "Dislocation Models of Crystal Grain Boundaries," *Phys. Rev.*, **78** [3] 275–89 (1950).
- ⁷F. C. Frank, "The Resultant Content of Dislocations in an Arbitrary Intercrystalline Boundary"; pp. 151–54 in *A Symposium on the Plastic Deformation of Crystalline Solids*. Office of Naval Research, Washington, DC, 1950.
- ⁸C. Herring, "Surface Tension as a Motivation for Sintering"; pp. 143–79 in *The Physics of Powder Metallurgy*. Edited by W. E. Kingston. McGraw-Hill, New York, 1951.
- ⁹A. Morawiec, "Method to Calculate the Grain Boundary Energy Distribution over the Space of Macroscopic Boundary Parameters from the Geometry of Triple Junctions," *Acta Mater.*, **48** [13] 3525–32 (2000).
- ¹⁰F. Williams, *Reasoning with Statistics*. Harcourt Brace Jovanovich, Fort Worth, TX, 1992.
- ¹¹D. M. Saylor and G. S. Rohrer, "Evaluating Anisotropic Surface Energies Using the Capillarity Vector Reconstruction Method," *Interface Sci.*, **9** [1/2] 35–42 (2001).
- ¹²D. Wolf, "Correlation Between Structure, Energy, and Ideal Cleavage Fracture for Symmetrical Grain Boundaries in fcc Metals," *J. Mater. Res.*, **5** [8] 1708–30 (1990). □